Nuclear Engineering and Design 100 (1987) 255–262
North-Holland, Amsterdam

THE COUNTERGRADIENT HEAT FLUX IN TURBULENT STRATIFIED FLOWS *

U. SCHUMANN

DFVLR, Institute of Atmospheric Physics, D-8031 Oberpfaffenhofen, Fed. Rep. Germany

Received 25 September 1986

Countergradient heat flux (CGHF) transports heat from low to high temperature regions. The reasons for this paradoxial behaviour are explained in this paper. We report on three examples for which CGHF has been observed either experimentally or in direct numerical simulations. The examples concern vertical heat flux in convective or stably stratified layers with or without shear. It is shown that CGHF arises in stably stratified parts of the flow if the dissipation of temperature fluctuations is too small to balance source terms for such fluctuations. In such cases, CGHF converts potential energy into kinetic energy. By means of an eigenanalysis of a second order model we support this explanation and show that CGHF appears in particular for high Prandtl number flows.

1. Introduction

Turbulence is an important process in many applications, be it nuclear engineering or atmospheric physics. The common understanding of turbulence is that turbulence mixes momentum or temperature fields much more effectively than molecular diffusion. Classical gradient transport models describe turbulence like molecular mixing with the molecular diffusivity replaced by an effective turbulent diffusivity. A prominent example of such models is the Prandtl mixing-length model. This class of models always assumes that temperature, e.g., is transported down the gradient from regions with high temperature to regions with low temperature. Such models cannot account for cases in which turbulence transports heat counter the gradient of temperature from low to high temperature regions.

Starr [1] has described several examples from geo- and astrophysics where momentum or heat is transported counter the gradient. He gives qualitative explanations of this effect and shows that countergradient fluxes are indications for exchange between different forms of energy. Deardorff [2] shows that countergradient heat flux arises in the lower atmosphere and in laboratory experiments and explains this effect in terms of the second-order equations for temperature variance. He shows that vertical diffusion of such variance is responsible for countergradient heat flux in these cases. Komori et al. [3] found countergradient heat flux in stably stratified, quasi homogeneous turbulence. In this case diffusional transport effects are small and cannot be the reason for the effect therefore. Komori et al. explain the effect in terms of wave pumping.

In this paper three examples of countergradient heat flux ("CGHF") in stratified flows are reported and its origin is explained in a unified manner. The examples concern vertical heat flux in buoyant or stably stratified layers, with or without shear, being either homogeneous or inhomogeneous. The examples are based on previous laboratory or numerical investigations of the turbulent flow fields [3–9]. Here, the results are supported by applying a second-order closure model which allows to determine quasi-steady flow states in a decaying turbulence.

It will be shown that a CGHF arises if dissipation of temperature fluctuations is too small to balance sources of such fluctuations. This leads to the hypothesis that CGHF is typical for high Prandtl number flows where conductive dissipation of temperature variance is small. Indeed it will be shown that a CGHF is turned to standard gradient heat-flux if the Prandtl number is reduced.

2. Examples of countergradient heat flux

2.1. Stratified turbulent shear flow

Komori, Ueda, Oginu and Mizushina [3] measured turbulence intensities and fluxes in stably stratified

* Dedicated to Prof. Dr. D. Smidt on the occasion of his 60th birthday.

shear flow. The shear flow was generated by the flow of water in a flat channel. The water in the open channel was heated from above by condensing steam. This resulted in a flow with Richardson number

$$\mathrm{Ri} = \alpha g (\mathrm{d}T/\mathrm{d}z)(\mathrm{d}U/\mathrm{d}z)^{-2} \geq 0$$

varying between about zero at the bottom of the channel and one near the surface. Here $\alpha = -\rho_0^{-1}(\partial\rho/\partial T)$ is the volumetric expansion coefficient, $\mathrm{d}T/\mathrm{d}z$ and $\mathrm{d}U/\mathrm{d}z$ are the vertical temperature and velocity gradients. The coordinates are x in the direction of the flow with mean velocity U, y is the cross-stream direction and z is pointing vertically upwards. The corresponding time-dependent turbulent velocity-fluctuations are u, v and w. Brackets $\langle\ \rangle$ denote ensemble averages and primes as in u' denote root-mean-square fluctuations.

For low Richardson numbers, the measurements, see fig. 1, resulted in negative turbulent heat fluxes $\langle wT \rangle$ in the vertical direction, which is consistent with a gradient transport model. For large Richardson-numbers, $\mathrm{Ri} > 0.5$, however, the heat flux changes sign so that a CGHF appears.

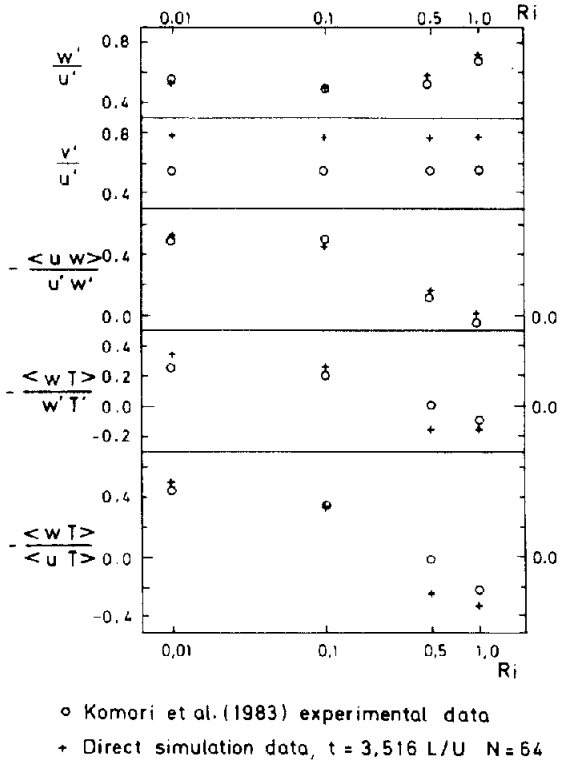

Fig. 1. Turbulence fluctuations and fluxes versus local gradient Richardson number, comparison of measurements (○) of Komori et al. [3] with results of a direct numerical simulation (+) [5]. The brackets $\langle\ \rangle$ denote ensemble averages, the primes denote root-mean-square values.

Komori et al. showed that these tendencies are qualitatively in agreement with the results of a linear spectral model of homogeneous turbulence. They conclude that intermittent upward motions of advected eddies with positive spikes of temperature fluctuations cause upward heat flux against the temperature gradient. The intermittent spikes are attributed to the observed wavelike motion under stable stratification.

We note that the magnitude of the heat flux in horizontal direction $\langle uT \rangle$ is comparable with the vertical heat flux although the horizontal gradient of mean temperature is negligible. This is another example where gradient models fail.

Elghobashi, Gerz and Schumann [4,5] have performed direct simulations of turbulence under conditions which represent a small cube inside the water channel investigated by Komori et al. [3]. The cube with side length L is taken to be large enough in order to capture all energy containing eddies but small in comparison to the depth of the water channel so that the flow can be approximately considered as being homogeneous in all space directions.

The simulation scheme uses a combined finite-difference and pseudo-spectral method to numerically integrate the full three-dimensional Navier–Stokes equations on a 64^3 grid. Periodic boundary conditions are used in the horizontal directions (x–y), and "shear-periodic" boundary conditions in the vertical [5].

The parameters of the simulation (to which we refer later again) are:

- Reynolds number $\mathrm{Re} = uL/\nu = 58050$
- Prandtl number $\mathrm{Pr} = \nu/\gamma = 5$ (water)
- Shear number $\mathrm{Sh} = (\mathrm{d}U/\mathrm{d}z)l/v = 4$
- Taylor micro-scale $\lambda/L = 0.026$
- Richardson-number $\mathrm{Ri} = \alpha g \Delta T L/U^2 = 0$ to 1

Here L is the size of the computational domain, $U = L|\mathrm{d}U/\mathrm{d}z|$, $\Delta T = L|\mathrm{d}T/\mathrm{d}z|$, l is the integral length scale of turbulence, and v the root-mean-square velocity fluctuation.

Starting from random initial conditions, integration is performed until a quasi-stationary state is reached for which correlation coefficients like $\langle wT \rangle/(w'T')$ become approximately steady.

The results are shown together with the measurements of Komori in fig. 1. The general agreement supports the validity of the simulation. Both, experiment and simulation show negative values of

$-\langle wT\rangle/(w'T')$, i.e. a CGHF, for strong stable stratification with $\mathrm{Ri} \geq 0.5$. Since the simulation applies for homogeneous conditions, the results show that a CGHF arises also for purely homogeneous flows without any advective or diffusive sources.

2.2. *Internally heated fluid layer*

Grötzbach [6] numerically simulated the turbulent flow in a channel between two horizontal plane walls driven by a spatially constant internal heat source. The heat is transferred to the walls which are kept at constant temperature. The numerical simulation integrates the Navier–Stokes equations on a finite difference grid with $64 \times 64 \times 32$ grid points. The simulation mimics heat removal from molten fluid of nuclear reactors and for this purpose the Prandtl number is set to $\mathrm{Pr} = 6$.

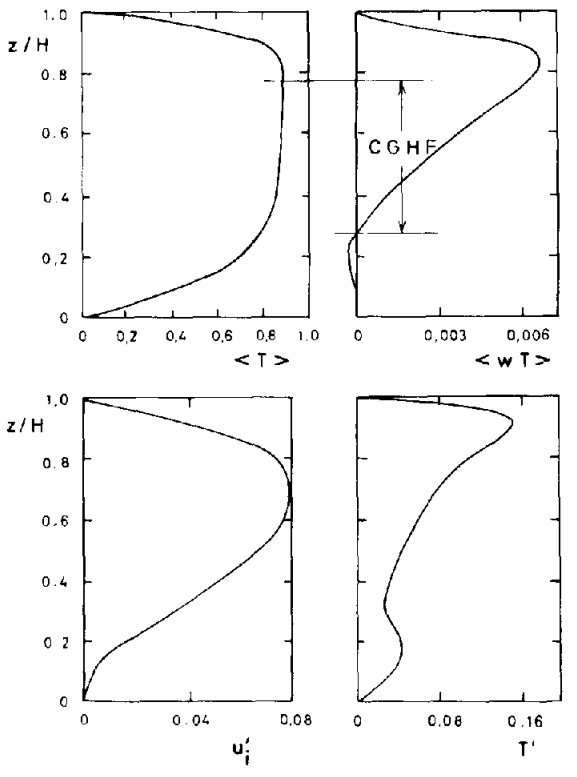

Fig. 2. Profile of mean temperature $\langle T\rangle$, vertical heat flux $\langle wT\rangle$, root-mean-square (r.m.s.) velocity fluctuations, $u_i' = \langle u_i^2\rangle^{1/2}$, and r.m.s. temperature fluctuations T' versus vertical coordinate z (normalized by channel height H) in an internally heated fluid layer [6]. The region with countergradient heat flux (CGHF) is indicated.

The Rayleigh number is 107 times the critical one. The simulation is run over a long integration time so that the results can be considered as stationary. Some of the resultant vertical profiles of horizontally averaged quantities are reproduced in fig. 2. Grötzbach showed that the resultant heat flux at the walls, the maximum temperature, and the spatial structure of the convective motion does well agree with available experimental data.

The internal heating results in a vertical temperature profile with a maximum at $z/H \approx 0.75$ where H is the channel height, $z = 0$ at the lower wall, $z = H$ at the top wall. So the fluid is stably stratified for $z < 0.75H$. The vertical turbulent heat flux $\langle wT\rangle$ is positive for $z > 0.27H$ and negative below. Thus we find CGHF in the region $0.27 < z/H < 0.75$.

As will be seen later it is important to note, that the kinetic energy of turbulence is large in the interior domain with a maximum at $z/H \approx 0.7$, while the temperature fluctuations have a local minimum at $z/H \approx 0.3$, i.e. near the position where $\langle wT\rangle$ vanishes.

2.3. *Convective boundary layer*

The convective atmospheric boundary layer is observed over warm surfaces for small wind speeds. It can be considered as an initially stably stratified fluid layer heated from below. The heat supply drives convective turbulent motion in the boundary layer up to an inversion height H which gradually entrains into the stable layer aloft. The flow is time-dependent but profiles normalized with the inversion height H behave quasi stationary.

This flow has been investigated experimentally by Deardorff and Willis [7] in a laboratory experiment using a water tank heated from below. The situation has been analysed with second-order turbulence models by Finger and Schmidt [8], see fig. 3. Model M1 uses the full second order equations with parametrisations for third order moments. Model M2 uses the second-order equations with algebraic approximations, i.e. neglects the time differentials and diffusional transports of the anisotropic parts of the second-order moments. Preliminary results of a large-eddy simulation for this case [9] support the results of model M1.

Experiment and theory show that the turbulent vertical heat-flux is positive from the ground up to a height $z/H \approx 0.8$ but the temperature gradient is more or less zero or even slightly positive for approximately $z/H > 0.4$ indicating stable stratification. Again, this is an example of CGHF in the domain $0.4H < z < 0.8H$. Note that model M2 does not predict a CGHF.

The kinetic energy is large inside the boundary layer

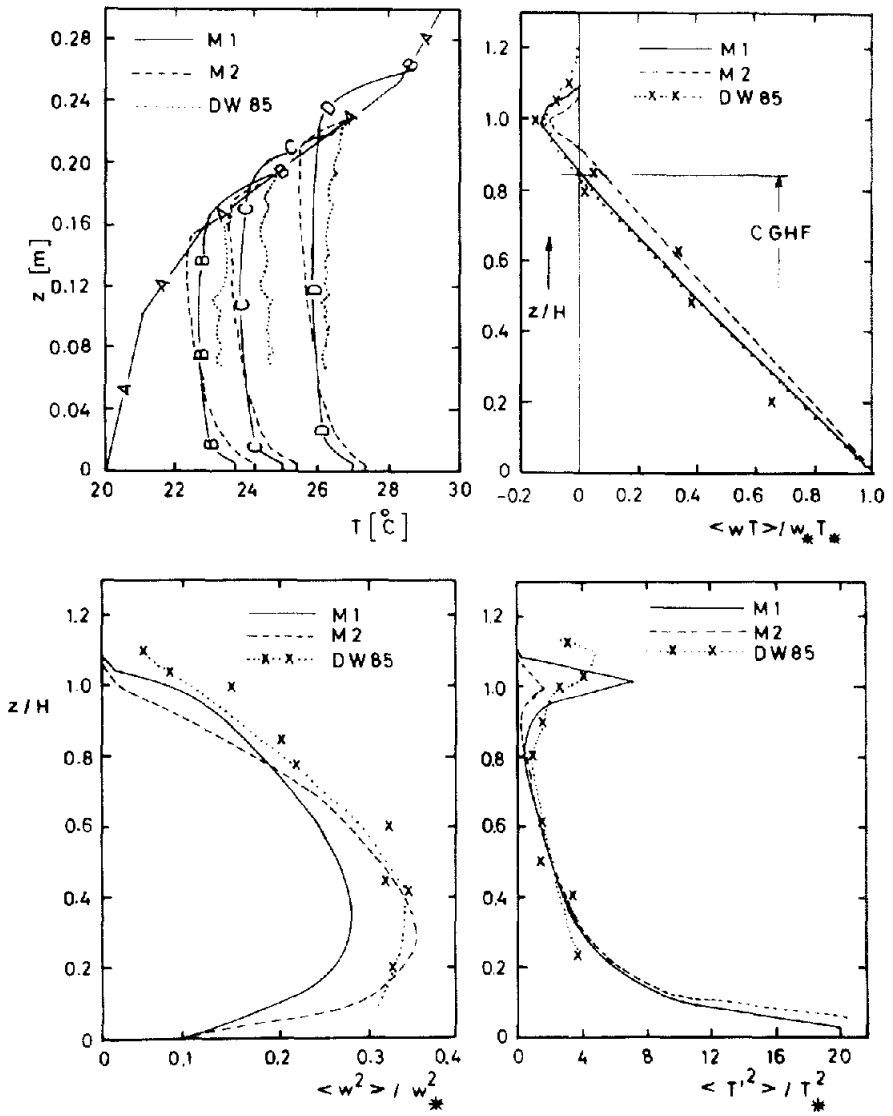

Fig. 3. Profiles of mean temperature $\langle T \rangle$, at a sequence of times A–D, vertical heat flux $\langle wT \rangle$, vertical velocity variance $\langle w^2 \rangle$ and temperature variance $\langle T^2 \rangle$ versus vertical coordinate z (H = inversion height) in a convective boundary layer using convective scales [8]. The curves represent results from models M1 and M2 and experimental data from Deardorff and Willis (DW) [7]. The region with CGHF extends down to the position of minimum mean temperature (not measured).

with a maximum at $z/H = 0.3$. The temperature fluctuations are large near the ground and near the inversion height but show a pronounced local minimum near $z/H \simeq 0.8$ where the heat flux vanishes. We will see that this is typical for the appearance of CGHF.

As mentioned in the introduction, Deardorff [2] has explained the appearance of CGHF for this case. The subsequent discussion generalizes his explanation.

3. Discussion using second-order closure models for homogeneous stratified turbulence

3.1. Interpretation of the unclosed equations

From the Navier–Stokes equations (including the first law of thermodynamics for heat transport) one can deduce transport equations for the Reynolds stresses

$\langle u_i u_j \rangle$, temperature fluxes $\langle u_i T \rangle$, with $u_i = (u, v, w)$, and the temperature variance $\langle T^2 \rangle$ [10,11].

Especially for homogeneous stratified turbulence with uniform shear $\mathrm{d}U/\mathrm{d}z$ and temperature gradient $\mathrm{d}T/\mathrm{d}z$ these equations, normalized by reference scales L, U and $\Delta T > 0$, are given below:

$$\partial\langle u^2\rangle/\partial t = -2S\langle uw\rangle + \Phi_{11} - \epsilon_{11}, \tag{1a}$$

$$\partial\langle v^2\rangle/\partial t = \quad + \Phi_{22} - \epsilon_{22}, \tag{1b}$$

$$\partial\langle w^2\rangle/\partial t = 2\,|\mathrm{Ri}|\langle wT\rangle + \Phi_{33} - \epsilon_{33}, \tag{1c}$$

$$\partial\langle uw\rangle/\partial t = -S\langle w^2\rangle + |\mathrm{Ri}|\langle uT\rangle + \Phi_{13} - \epsilon_{13}, \tag{1d}$$

$$\partial\langle uT\rangle/\partial t = -s\langle uw\rangle - S\langle wT\rangle + \Phi_{1T} - \epsilon_{1T}, \tag{1e}$$

$$\partial\langle wT\rangle/\partial t = -s\langle w^2\rangle + |\mathrm{Ri}|\langle T^2\rangle + \Phi_{3T} - \epsilon_{3T}, \tag{1f}$$

$$\partial\langle T^2\rangle/\partial t = -2s\langle wT\rangle - \epsilon_{TT} + q. \tag{1g}$$

Here the following abbreviations [10,11] are used:

$\mathrm{Ri} = s\alpha g L\Delta T/U^2$,
Φ_{ij} = redistribution of $\langle u_i u_j \rangle$ by pressure fluctuations,
Φ_{jT} = redistribution of $\langle u_j T \rangle$ by pressure fluctuations,
ϵ_{ij} = dissipation rate of $\langle u_i u_j \rangle$,
ϵ_{jT} = dissipation rate of $\langle u_j T \rangle$,
ϵ_{TT} = dissipation rate of $\langle T^2 \rangle$,
$S = (L/U)\mathrm{d}U/\mathrm{d}z$ (non-dimensional shear),
$s = (L/\Delta T)\mathrm{d}T/\mathrm{d}z$ (non-dimensional stratification).

The source term q for temperature-variance in eq. (1g) has been included for later discussion of the effect of such sources. For homogeneous turbulence, $q \equiv 0$.

These equations require closure assumptions for several terms if one wants to use them for predictions. However, already without closure the equations allow to explain the occurrence of CGHF:

As has been noted by Deardorff [2], eq. (1g), the balance for temperature variance is of particular importance. It can be solved for the vertical turbulent heat flux:

$$\langle wT\rangle = -\big(\epsilon_{TT} + \partial\langle T^2\rangle/\partial t - q\big)/(2s). \tag{2}$$

Here $s = 1$ for stable stratification and $\epsilon_{TT} > 0$ because the molecular dissipation rate is a positive definite.

From eq. (2) it follows that for stationary and stably stratified turbulence and in the absence of external sources for temperature variance, $q = 0$, the heat flux $\langle wT \rangle$ is always negative. Thus the heat flows down the gradient under these conditions. However, the heat flux may change sign and become a CGHF if $\partial\langle T^2\rangle/\partial t < -\epsilon_{TT}$ or if a strong positive source q is imposed.

Obviously, the experiment of Komori and the related simulations of Elghobashi, Gerz and Schumann are cases with $q = 0$ but $\partial\langle T^2\rangle/\partial t < -\epsilon_{TT}$. Thus CGHF arises here if the dissipation rate is too small to balance the source from the reservoir of temperature variance. In this case, the dissipation ϵ_{TT} is small because of the large Prandtl number fluid and relatively small Reynolds number, see below.

The internally heated layer considered by Grötzbach and the atmospheric boundary layer are examples where the CGHF is due to large diffusional sources q of temperature variance in stationary turbulence. Such diffusional sources are likely to exist in these cases because the temperature variance, see figs. 2 and 3, shows a local minimum in the region with CGHF. The reason for this local minimum can also be understood from eq. (1g). $\langle T^2 \rangle$ gets small where $s\langle wT \rangle$ takes its minimum. Since $s > 0$, this is the case near the position of minimum heat flux $\langle wT \rangle$. Also the turbulence intensity is large here so that turbulence effectively diffuses variance into the domain where the CGHF is observed. Hence, CGHF in these cases results because the dissipation rate ϵ_{TT} is too small to balance diffusional sources. This explanation is further supported by Finger&Schmidt [8] who found that the CGHF disappears if the diffusion terms are neglected. This can be seen from fig. 3 for model M2.

Since eqs. (1) are a pure consequence of the averaged Navier–Stokes equations (including the first law of thermodynamics) without any closure assumptions we conclude that CGHF is consistent with the Navier–Stokes equations.

Moreover, we can understand the effect on the basis of energy considerations for stable stratification ($s = 1$, $\mathrm{Ri} > 0$). The total turbulence energy is the sum of kinetic energy plus potential energy $\frac{1}{2}g\langle \rho' h' \rangle$ [12]. here h' is the vertical displacement of a fluid parcel with density deviation ρ'. Using

$$\rho' = (\partial\rho/\partial T)T' = -\alpha T'\rho_0,$$

$$h' = -(\mathrm{d}T/\mathrm{d}z)^{-1}T',$$

we obtain for the total turbulence energy k_{tot} in nondimensional units:

$$k_{\mathrm{tot}} = \big(\langle u^2\rangle + \langle v^2\rangle + \langle w^2\rangle + \mathrm{Ri}\langle T^2\rangle\big)/2. \tag{3}$$

From eqs. (1), i.e. for homogeneous turbulence, we obtain (with $\epsilon \equiv \frac{1}{2}\epsilon_{ii}$):

$$\partial k_{\mathrm{tot}}/\partial t = -S\langle uw\rangle - \epsilon - \mathrm{Ri}\epsilon_{TT}/2. \tag{4}$$

Thus, the total turbulence energy in homogeneous turbulence is insensitive to the heat flux $\langle wT \rangle$. The heat flux has the function of converting energy from kinetic to potential ($\langle wT \rangle < 0$) or vice-versa ($\langle wT \rangle > 0$). (For inhomogeneous cases diffusional sources will

contribute to the energy balance.)

Under quasi-stationary conditions the ratio of potential to kinetic energy should be constant. If, however, dissipation of temperature variance ϵ_{TT} is large in comparison to mechanical dissipation ϵ than an imbalance arises and the fraction of potential energy becomes too small. In this case $\langle wT\rangle < 0$ is required to create additional potential energy for equilibrium. On the other hand, if ϵ_{TT} is small, then the CGHF serves to recreate the equilibrium. Thus a CGHF is energetically consistent.

3.2. A second-order closure model and its results

Subsequently we use closure models for the redistribution and dissipation terms. The closure is based on the proposals of Launder [10,11] with extensions to account for viscous and conductive dissipation as required for moderate Reynolds numbers. The model is linearized by keeping the frequency scale $\tau^{-1} = \epsilon/k$ of turbulent redistribution and dissipation constant. Also nonlinear contributions [11] for Φ_{iT} are neglected. The closure model reads as follows:

$$\begin{aligned}
\Phi_{11} &= -c_1\tau^{-1}\left(\langle uu\rangle - \tfrac{2}{3}k\right) + c_2\tfrac{4}{3}\langle uw\rangle S \\
&\quad + \tfrac{2}{3}c_3|\mathrm{Ri}|\langle wT\rangle, \\
\Phi_{22} &= -c_1\tau^{-1}\left(\langle vv\rangle - \tfrac{2}{3}k\right) - c_2\tfrac{2}{3}\langle uw\rangle S \\
&\quad + \tfrac{2}{3}c_3|\mathrm{Ri}|\langle wT\rangle, \\
\Phi_{33} &= -c_1\tau^{-1}\left(\langle ww\rangle - \tfrac{2}{3}k\right) - c_2\tfrac{2}{3}\langle uw\rangle S \\
&\quad - \tfrac{4}{3}c_3|\mathrm{Ri}|\langle wT\rangle, \\
\Phi_{13} &= -c_1\tau^{-1}\langle uw\rangle + c_2\langle ww\rangle S - c_3|\mathrm{Ri}|\langle uT\rangle, \\
\Phi_{1T} &= -c_{1T}\tau^{-1}\langle uT\rangle + 0.8\langle wT\rangle S, \\
\Phi_{3T} &= -c_{1T}\tau^{-1}\langle wT\rangle - 0.2\langle uT\rangle S \quad c_{2T}|\mathrm{Ri}|\langle T^2\rangle.
\end{aligned} \tag{5}$$

$$\begin{aligned}
\epsilon_{11} &= \tfrac{2}{3}\tau^{-1}k + c_\epsilon\left(\nu'/\lambda^2\right)\langle uu\rangle, \\
\epsilon_{22} &= \tfrac{2}{3}\tau^{-1}k + c_\epsilon\left(\nu'/\lambda^2\right)\langle vv\rangle, \\
\epsilon_{33} &= \tfrac{1}{3}\tau^{-1}k + c_\epsilon\left(\nu'/\lambda^2\right)\langle ww\rangle, \\
\epsilon_{13} &= c_\epsilon\left(\nu'/\lambda^2\right)\langle uw\rangle, \\
\epsilon_{1T} &= c_\epsilon\left(\tfrac{1}{2}(\nu'+\gamma')/\lambda^2\right)\langle uT\rangle, \\
\epsilon_{3T} &= c_\epsilon\left(\tfrac{1}{2}(\nu'+\gamma')/\lambda^2\right)\langle wT\rangle, \\
\epsilon_{TT} &= \tau^{-1}\mathrm{Pr}_t^{-1}\langle T^2\rangle + c_\epsilon\left(\gamma'/\lambda^2\right)\langle T^2\rangle,
\end{aligned} \tag{6}$$

$$k = \left(\langle u^2\rangle + \langle v^2\rangle + \langle w^2\rangle\right)/2, \tag{7}$$

$$\tau^{-1} = \tfrac{2}{5}^{1/2}c_d/\mathrm{Sh} = \epsilon/k.$$

The model coefficients are

$$c_1 = 2.0, \quad c_2 = 0.6, \quad c_3 = 0.3, \quad c_{1T} = 3.2, \quad c_{2T} = 0.5,$$
$$c_\epsilon = 10.0, \quad c_d = 0.7.$$

Other model parameters are taken in order to model the experiment of Komori according to section 2.1.

$$\lambda = 0.025, \quad \nu'^{-1} = \mathrm{Re} = 58050, \quad \nu'/\gamma' \equiv \mathrm{Pr} = 5,$$
$$\mathrm{Sh} = 4, \quad 0 \le \mathrm{Ri} \le 1.$$

It turned out that the results of the model are rather sensitive to c_ϵ and λ, i.e. with respect to the viscous and conductive dissipation terms. Rather arbitrarily we assume $\mathrm{Pr}_t = 1$.

The resulting set of equations can be written in matrix form

$$\partial \boldsymbol{a}/\partial t = \boldsymbol{A}\boldsymbol{a}, \tag{8}$$

where

$$\boldsymbol{a}^{\mathrm{T}} = \langle(u^2, v^2, w^2, uw, uT, wT, T^2)\rangle, \tag{9}$$

and $\boldsymbol{A}$ is a constant matrix because we assumed ϵ/k to

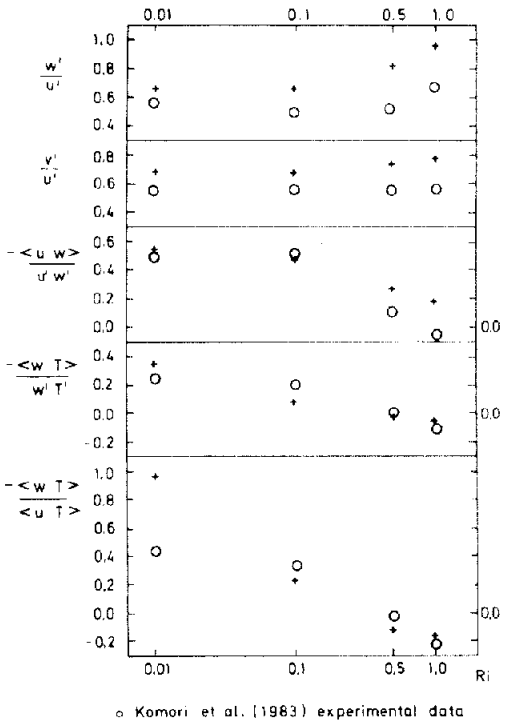

Fig. 4. As fig. 1 but results of a second-order closure model (+) in comparison to the measurements (○) of Komori et al [3].

be prescribed as a function of the shear number. For solution, we employ

$$\boldsymbol{a} = \boldsymbol{x}\, e^{\lambda t}. \tag{10}$$

This results in an eigenvalue-problem,

$$\boldsymbol{A}\boldsymbol{x} = \lambda \boldsymbol{x}. \tag{11}$$

The eigenvector $\boldsymbol{x}$ corresponding to the eigenvalue with maximum real part is the least damped mode and therefore determines the amplitudes of the quasi-stationary solution. It turned out that this particular eigenvalue is always real. This approach gives results which are independent of arbitrarily selected initial values.

The results are plotted in fig. 4, again in comparison to the values measured by Komori et al. The agreement is not quite as good as in fig. 1. However, the general trends including the appearance of the CHGF are well predicted. Also the initial decrease of w'/u' and later increase versus Ri-number is represented by the model. It is interesting to note that both the direct simulation and the second-order model give much larger values for the ratio v'/u' than the experiment. This suggests deficiencies in the measurements. The comparison shows that the present model can serve to investigate the effect of model parameters on the vertical heat flux correlation coefficient.

Our explanation of CGHF as given in section 3.1 suggests that a CGHF arises if the dissipation rate ϵ_{TT} is small in comparison to other contributions to the balance for temperature variance. For small to moderate Reynolds numbers, the rate ϵ_{TT} is reduced if the Prandtl-number Pr becomes large. Therefore, the second-order model has been applied for various values of the Prandtl-number. Fig. 5 shows that the CGHF indeed disappears for small Prandtl-numbers and is enforced for large Prandtl-numbers. For larger Reynolds numbers the flow becomes likewise sensitive to the turbulent Prandtl number. This is consistent with the explanations given in section 3.1.

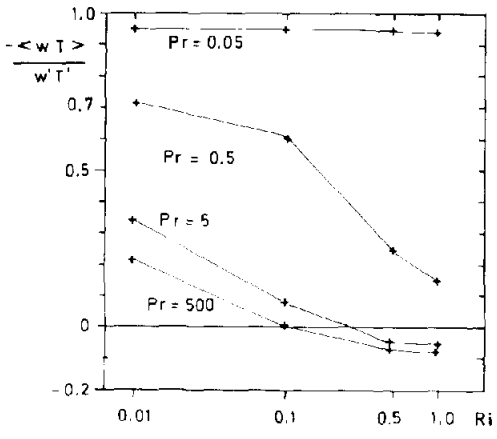

Fig. 5. Effect of Prandtl number on the heat flux correlation coefficient versus Richardson number as computed with the second-order closure model.

4. Conclusions

Three examples of turbulent flows with countergradient heat flux (CGHF) have been reported. Both laboratory experiments and direct numerical simulations show that such a CGHF exists. From investigations of second-order model equations formed from the Navier–Stokes equations and on the basis of energy considerations the following reasons have been identified to cause CGHF:

CGHF appears in stably stratified turbulence if the dissipation of temperature fluctuations is too small to balance source terms which might result from either diffusional transports or a reservoir of temperature fluctuations in decaying turbulence. In these cases the CGHF converts potential energy into kinetic energy which is then mechanically dissipated. Thus CGHF is both consistent with the Navier-Stokes equations and with energy considerations.

Explanations in terms of intermittent wave-pumping [3] or 'bubbles' of warm fluid penetrating inversion layers give additional insights in the motion mechanisms but are not necessary to explain the origin of CGHF.

Increasing the dissipation of temperature variance reduces the appearance of CGHF. For moderate Reynolds numbers where direct conductive and viscous dissipation rates are large in comparison to inertial dissipation rates such an increase of temperature-variance dissipation can be achieved by lowering the Prandtl number. This has been shown by means of a second order closure model.

In summary, the origin of countergradient heat flux in stratified turbulence has been explained.

Acknowledgement

I thank Prof. S.E. Elghobashi, Th. Gerz, Dr. G. Grötzbach, J. Finger, and H. Schmidt for permission to reproduce some of their figures and for valuable suggestions on a draft of this paper. Part of this work has been supported by the Deutsche Forschungsgemeinschaft.

References

[1] V. Starr, Physics of Negative Viscosity Phenomena (McGraw-Hill Book Co., New-York, 1968).

[2] J.W. Deardorff, The counter-gradient heat flux in the lower atmosphere and in the laboratory, J. Atmosph. Sci. 23 (1966) 503–506.

[3] S. Komori, H. Ueda, F. Ogino and T. Mizushina, Turbulence structure in stably stratified open-channel flow, J. Fluid Mech. 130 (1983) 13–26.

[4] S.E. Elghobashi, T. Gerz and U. Schumann, Direct simulation of turbulent homogeneous shear flow with buoyancy, Proc. 5th Symp. on Turbulent Shear Flows, Aug. 7–9, 1985, Cornell Univ., Ithaca, New York, pp. 22.7–22.12 (1985).

[5] U. Schumann, S.E. Elghobashi and T. Gerz, Direct simulation of stably stratified turbulent homogeneous shear flows, in: U. Schumann and R. Friedrich, eds.: Direct and Large Eddy Simulation of Turbulence. Notes on Numerical Fluid Mechanics, Vol. 15 (Vieweg-V., Braunschweig, 1986) 245–264.

[6] G. Grötzbach, Direct numerical and large eddy simulation of turbulent channel flows, in: N.P. Cheremisinoff, ed.: Encyclopedia of Fluid Mechanics, Vol. 6 (Gulf Publ., West Orange, NJ, 1986).

[7] J.W. Deardorff and G.E. Willis, Further results from a laboratory model of the convective planetary boundary layer, Boundary-Layer Meteor. 32 (1985) 205–236.

[8] J.E. Finger and H. Schmidt, On the efficiency of different higher order turbulence models simulating the convective boundary layer, Beitr. Phys. Atmosph. 59 (1986) 505–517.

[9] H. Schmidt, J.E. Finger and U. Schumann, Comparison of large eddy simulations of a convective layer with one-dimensional models, Conf. EGS/ECS Kiel, 21.–30.8.1986, Abstract in Terra cognita 6 (1986) No. 3, 450.

[10] B.E. Launder, On the effects of a gravitational field on the turbulent transport of heat and momentum, J. Fluid Mech. 67 (1975) 569–581.

[11] B.E. Launder, Heat and mass transport, in: P. Bradshaw, ed.: Turbulence – Topics in Applied Physics, Vol. 12 (Springer-V., Berlin, 1978), 232–287.

[12] J.J. Riley, R.W. Metcalfe, M.A. Weissman, Direct numerical simulations of homogeneous turbulence in density-stratified fluids, in: B.J. West, ed.: Nonlinear Properties of Internal Waves (Amer. Inst. Phys., New York, 1981) 79–112.